SCIENTIFIC REP🔴RTS

OPEN

Polyamorphism in Yb-based metallic glass induced by pressure

HPSTAR
481-2017

Liangliang Li[1,2], Qiang Luo[3], Renfeng Li[1,2], Haiyan Zhao[4,5], Karena W. Chapman[5], Peter J. Chupas[5], Luhong Wang[1] & Haozhe Liu[1,2]

The $Yb_{62.5}Zn_{15}Mg_{17.5}Cu_5$ metallic glass is investigated using synchrotron x-ray total scattering method up to 38.4 GPa. The polyamorphic transformation from low density to high density with a transition region between 14.1 and 25.2 GPa is observed, accompanying with a volume collapse reflected by a discontinuousness of isothermal bulk modulus. This collapse is caused by that distortional icosahedron short range order precedes to perfect icosahedron, which might link to Yb 4f electron delocalization upon compression, and match the result of *in situ* electrical resistance measurement under high pressure conditions. This discovery in Yb-based metallic glass, combined with the previous reports on other metallic glass systems, demonstrates that pressure induced polyamorphism is the general behavior for typical lanthanide based metallic glasses.

Traditional network-forming glassy state materials[1], such as ice[2], silica[3] and silicon[4] have been reported to exhibit polyamorphism induced by pressure, which tends to be ascribed to an increase in atomic coordination. Whereas, metallic glasses are distinct from the traditional glasses due to the non-directional metallic bonds. Therefore, polyamorphism induced by pressure in metallic glass was supposed to be impossible for they are spatially densely-packing and have the maximum coordination number already. However, polyamorphic transitions were discovered in Ce-based metallic glasses attributed to 4f electron delocalization in Ce under high pressure[5,6]. This rises a question that it is the general behavior for all lanthanide based metallic glasses, or not.

Ytterbium, as an end member of the rare-earth lanthanides, behaves irregular in comparison with other members of the lanthanide series owing to its special electronic configuration. At ambient conditions, ytterbium is considered as divalent with an electronic configuration close to $4f^{14}(5d6s)^2$, while the other lanthanides as trivalent state $4f^n(5d6s)^3$, where n varies from 0 to 14 corresponding to lanthanum to lutetium. The special electronic configuration of ytterbium results in a special sequence of phase transitions at high temperatures as well as high pressures[7-10]. If Ce with electronic configuration of $4f^1(5d6s)^3$ could be looked as "n-type one electron" like beginning member, Yb, on the other hand, could be looked as $4f^{14}(5d6s)^{3+(-1)}$, i. e. "p-type one hole like" ending member, which indeed results in a d- rather than an f differentiating electron behavior. Therefore, searching the potential polyamorphic transformation in Yb-based metallic glasses under compression conditions will be interesting to reveal whether the generality of polyamorphism exists.

Generally, pressure-volume studies are particularly valuable in confirming whether polyamorphic transitions occur[10]. Such polyamorphic transformations derived from valence transitions should involve in changes of electrical transport property. In this work, to shed some light on the nature of polyamorphic transitions induced by pressure in Yb-based metallic glass systems, a study was performed by means of synchrotron x-ray total scattering and resistance measurements, focusing on another side of ending member of this lanthanide base metallic glass family, namely $Yb_{62.5}Zn_{15}Mg_{17.5}Cu_5$ metallic glass.

Results and Discussion

X-ray total scattering under pressure.
The structure factor $S(Q)$ and corresponding PDFs of the $Yb_{62.5}Zn_{15}Mg_{17.5}Cu_5$ metallic glass extracting from synchrotron x-ray scattering experiment as a function of pressure are displayed in Fig. 1. Absence of sharp peaks in $S(Q)$ and PDFs indicates that the sample remains fully amorphous state in the entire pressure range. As expected for the compression effect, first peak position Q_1 of structure factor $S(Q)$ in reciprocal space shifts towards higher momentum transfer and the nearest-neighbor

[1]Harbin Institute of Technology, Harbin 150080, China. [2]Center for High Pressure Science and Technology Advanced Research, Changchun 130015, China. [3]School of Materials Science and Engineering, Tongji University, Shanghai 201804, China. [4]Center for Advanced Energy Studies, University of Idaho, Idaho Falls, Idaho 83406, USA. [5]X-ray Science Division, Advanced Photon Source, Argonne National Laboratory, Argonne, Illinois 60439, USA. Correspondence and requests for materials should be addressed to L.W. (email: luhong1@hit.edu.cn) or H.L. (email: haozhe.liu@hpstar.ac.cn)
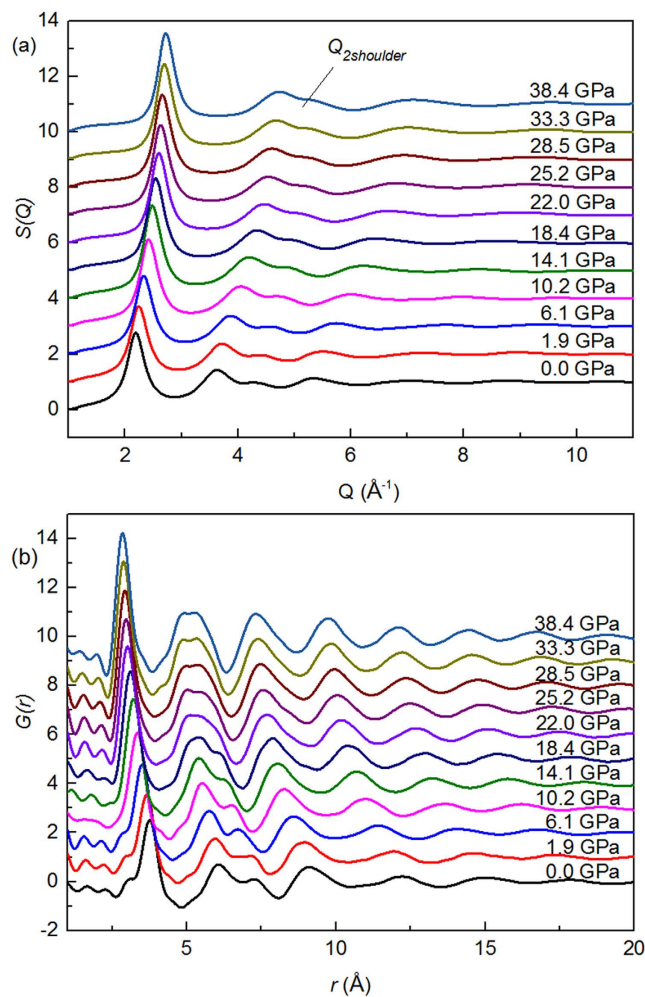
Figure 1. (**a**) Structure factor *S(Q)* and (**b**) pair distribution function *G(r)* of the $Yb_{62.5}Zn_{15}Mg_{17.5}Cu_5$ metallic glass at various pressure conditions.

distance r_1 in real space shifts to shorter distance with increasing pressure. The shifts of Q_1 of structure factor *S(Q)* and the nearest-neighbor distance r_1 reflect changes in volume or density induced by pressure, which is illustrated by a power law[3,11–13]. Using normalized first peak position Q_1 with a power of 2.5 to estimate the relative volume change as a function of pressure, a fast decrease of the average atomic volume under pressure range from 14.1 to 25.2 GPa, a transition region, is observed. Two amorphous states, low density amorphous states (LDAS) and high density amorphous states (HDAS), were separated by the transition region. Fitting the pressure-volume data by the second-order Birch-Murnaghan equation of state (EoS)[14], the isothermal bulk modulus are determined as $B_0 = 24(1)$ GPa and 45(7) GPa at different state region respectively, presenting a discontinuousness of isothermal bulk modulus, as shown in Fig. 2. The volume difference between the two states is as large as 15.2% at ambient pressure. Furthermore, the volume collapse taking place continuously and undergoing a broad pressure range rather than abruptly at certain pressure point shows an anomalous compressed region, which is in agreement with polyamorphic transition in $Ce_{55}Al_{45}$ metallic glass with a smooth and continuous transition region between 2 and 13.5 GPa[5]. This anomalous compressed curve is also observed in phase transition of ytterbium monotelluride under pressure[15].

As shown in Fig. 3(a,b), both Q_1 and r_1 move with a relatively fast pace at transition region and the changes of both Q_1 and r_1 as a function of pressure exhibit a trend similar to that of volume, which suggest that the poly-amorphic transformation is embodied as well in medium range and short range length scale besides long range length scale. Intuitive local structure change of $Yb_{62.5}Zn_{15}Mg_{17.5}Cu_5$ within short range length scale induced by pressure was reflected by gradually disappeared the low-r shoulder of the first peak in G(r), as shown in Fig. 1(b).

As is displayed in Fig. 1, the second peak in *S (Q)* and PDFs are of splitting at each pressure point which are characteristic for conventional amorphous alloy systems[16,17]. In real space, the changes splitting of second peak under pressure reflect structural changes of $Yb_{62.5}Zn_{15}Mg_{17.5}Cu_5$ in medium range length scale. Such change is consistent with phase transition characterized by shifts of Q_1 which embody the medium range order. In reciprocal space the relationship between the first peak and splitting second peak as a function of pressure is indicative of short range order change[18,19]. Define position of the second peak and its shoulder as Q_2 and $Q_{2shoulder}$. Using two

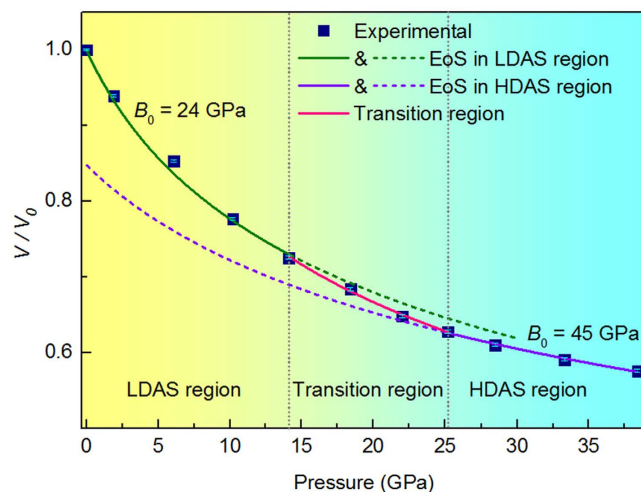**Figure 2. Relative volume V/V_0 of $Yb_{62.5}Zn_{15}Mg_{17.5}Cu_5$ metallic glass as a function of pressure, where V_0 is initial volume.** The green and purple line show the EoS fitting results at LDAS region and HDAS region, respectively. The pink line is for transition region.
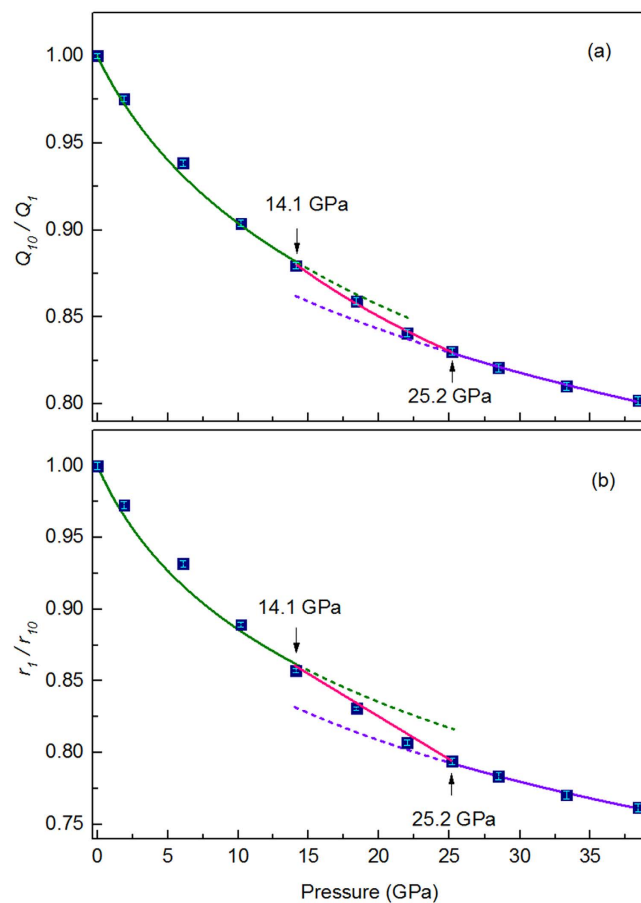

Figure 3. Pressure dependence of (**a**) normalized first peak position Q_1 and (**b**) normalized nearest-neighbor distance r_1, respectively, where Q_{10} and r_{10} are initial first peak position and nearest-neighbor distance, respectively. Equation used in fitting both Q_{10}/Q_1 and r_1/r_{10} as a function of pressure is based on second-order Birch-Murnaghan EoS.

Gaussian functions to fit the second peak, the ratios of peak position show $Q_{2shoulder}/Q_1 = 1.93$ and Q_2/Q_1 varying from 1.66 to 1.72 with increased pressure, as displayed in Fig. 4. In contrast to a perfect icosahedron short range order, $Q_{2shoulder}/Q_1 = 2.04$ and $Q_2/Q_1 = 1.71$[20], short range order changes in the $Yb_{62.5}Zn_{15}Mg_{17.5}Cu_5$ metallic glass
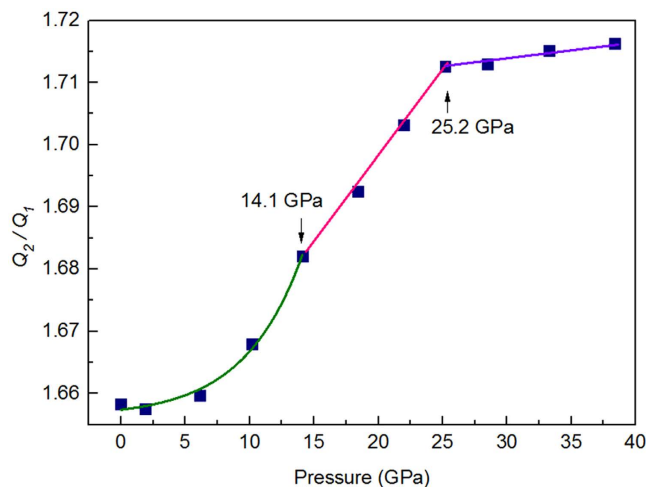
Figure 4. Q_2/Q_1 in the $Yb_{62.5}Zn_{15}Mg_{17.5}Cu_5$ metallic glass as a function of pressure.

under pressure go through from a more distortional icosahedra to a more perfect one with a different pace corresponding to different phase states. The polyamorphic transformation in the $Yb_{62.5}Zn_{15}Mg_{17.5}Cu_5$ metallic glass under pressure is thus mainly related to the reduction of icosahedra distortion with a different pace leading to volume collapse. This result is consistent with the change of PDFs whose each peak is sharper increasingly with increasing pressure, indicating the structure gradually becomes more order compared to initial structure, as presented in Fig. 1(b). At stage of LDAS, the change of distortion with pressure is slight and it contributes to a weak volume reduction. The diminution in degree of icosahedra distortion proceeds with faster pace within a transition region, then, distortional icosahedron is close to a more perfect one reaching the range of HDAS, which leads to a large volume change. Whereas, such changes of distortional icosahedra result from the decrease of average atomic distance in first neighbor shell with a different step as shown in Fig. 3(b), which should be radically associated with electronic transformation.

The phase transition of the $Yb_{62.5}Zn_{15}Mg_{17.5}Cu_5$ metallic glass can be ascribed to the electronic transition. In the $Yb_{62.5}Zn_{15}Mg_{17.5}Cu_5$ metallic glass, the $4f$ shell of Yb is completely full and considered as divalent with an electronic configuration close to $4f^{14}(5d6s)^2$ at ambient conditions, whereas, under high pressure conditions, it transforms to a trivalent state $4f^{13}(5d6s)^3$ when one of the localized $4f$ electrons is delocalized, which is deduced from mechanism lied in polymorphism in ytterbium compounds[9,21] and polyamorphism in Ce-based metallic glass under pressure[5,6]. An Yb in the trivalent state has a smaller atomic volume compared to divalent state, and this results in a striking decrease in average bond length, which coincides with the change of icosahedral distortion and volume collapse.

The pressure dependence of electrical resistivity.   Electronic transition in the $Yb_{62.5}Zn_{15}Mg_{17.5}Cu_5$ metallic glass should be reflected in changes of electronic transport property. Therefore, an *in situ* resistance measurement under compression conditions was carried out. Figure 5 displays the resistance of $Yb_{62.5}Zn_{15}Mg_{17.5}Cu_5$ metallic glass as a function of pressure. According to weak-scattering theory which is well suited for low-resistivity metallic glasses, the resistance of a metallic glass is considered as arising from disordered atom scattering described by structure factor[22,23]. The pressure dependence of electrical resistivity is effected by several factors, such as the Fermi energy, the electron-ion interaction and structure factor of the system. As a result of a rather delicate interplay of these factors, the resistivity of metallic glasses is either to increase or to decrease under compressed conditions depending on different systems[24,25]. In the $Yb_{62.5}Zn_{15}Mg_{17.5}Cu_5$ metallic glass system, a positive pressure coefficient of the resistivity (PCR) is observed. Additionally, both the structure and electronic transition are arising from Yb $4f$ electrons delocalization as well as relation between pressure and electrical resistivity is volume dependence[23], therefore, resistance of the $Yb_{62.5}Zn_{15}Mg_{17.5}Cu_5$ metallic glass exhibits a similar transition region, which is from 19.3 to 30.2 GPa, to that of low density to high density transition displayed in synchrotron x-ray scattering experiment. The shift of transition region might be due to quasi-hydrostatic pressure conditions in resistance measurement experiment. The pressure effect on this metallic glass is basically reversible, but with sluggish effect when pressure released. Thus this polyamorphism could only be studied *via in situ* high pressure methods.

The positive PCR obviously reduced after transition in the $Yb_{62.5}Zn_{15}Mg_{17.5}Cu_5$ metallic glass is observed in Fig. 5. Cheung and Ashcroft[26] found a positive PCR for the polyvalent metals Mg, Al, Sn and a negative PCR for the monovalent metal K in liquid metals under pressure. Particularly, the positive PCR is maximal for the divalent metals[22,25]. This conclusion may suit for Yb contribution to PCR of the $Yb_{62.5}Zn_{15}Mg_{17.5}Cu_5$ metallic glass as well. The conversion from divalent to trivalent Yb leads to that contribution of Yb to positive PCR in the $Yb_{62.5}Zn_{15}Mg_{17.5}Cu_5$ metallic glass decreases in case of $4f$ electron delocalization, which gives rise to decline of positive PCR after transition.

A polyamorphic transformation from low density to high density with a transition region between 14.1 and 25.2 GPa occurs accompanying with change of electrical transport property. The transitions could be explained
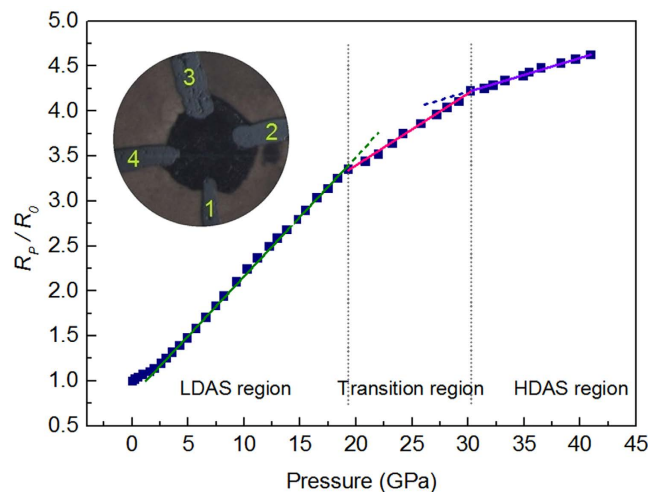
Figure 5. Relative resistance of the $Yb_{62.5}Zn_{15}Mg_{17.5}Cu_5$ metallic glass as a function of pressure. The inset shows the microphotograph of the sample with four Pt electrodes in chamber between two anvils at about 5 GPa conditions.

by $4f$ electron delocalization in Yb. The $4f$–$5d$ electronic collapse is reflected in both pressure-volume and pressure-resistivity relationship. This findings, combined with the previous reports on pressure induced poly-amorphism in Ce based and La based metallic glasses[5,6,17], is valuable to understand the polyamorphic transformation, which could be a general behavior in lanthanide based metallic glasses.

Methods

To achieve Yb-based metallic glasses with good glass forming ability, constituent elements Zn, Mg and Cu were carefully selected and adjusted the composition. Metallic glass $Yb_{62.5}Zn_{15}Mg_{17.5}Cu_5$ ribbons were prepared using the single-roller melt-spinning technique.

High-pressure PDF. Total synchrotron x-ray scattering data of the $Yb_{62.5}Zn_{15}Mg_{17.5}Cu_5$ metallic glass were collected at the sector 11-ID-B beamline at the Advanced Photon Source, Argonne National Laboratory with the incident beam size $150\,\mu m \times 150\,\mu m$ and an 86.7 keV high energy. A 2D large amorphous-silicon-based flat-panel detector was used to record the synchrotron x-ray scattering patterns. The sample with width of $150\,\mu m$, length of $150\,\mu m$ and thickness of $20\,\mu m$ was located in the sample chamber which is T301 stainless steel gasket with $270\,\mu m$ diameter hole between two anvils of diamond anvil cell (DAC). 1:4 methanol/ethanol and ruby are as pressure medium and marker, respectively. The pressure was up to 38.4 GPa and measured by the ruby fluorescence method with error bars of 0.1~0.2 GPa.

Raw image data were processed using software Fit-2D[27] with masking strategy[28] to remove the diamond peaks to obtain one-dimensional scattering data. Subtracting the contributions from the sample environment and background, the reduced pair distribution function $G(r)$ and structure factor $S(Q)$ were extracted using the program PDFgetX2[29], which carries out a numerical Fourier transform of $S(Q)$ according to

$$G(r) = \frac{2}{\pi} \int_0^\infty Q[S(Q) - 1]\,\sin(Qr)\,dQ. \tag{1}$$

High-pressure resistivity measurements. *In situ* electrical resistance was measured by a four-probe resistance system in a DAC. An aluminum oxide (Al_2O_3)/epoxy mixture powder layer was inserted between the T301 stainless steel gasket and diamond anvil to provide electrical insulation for the electrodes and gasket. Four electrodes made of platinum foil with a thickness of $10\,\mu m$ were arranged to contact the sample in the chamber. The pressure was determined by a ruby and up to 40.9 GPa. The resistance was calculated from the Van de Pauw method[30].

References

1. Vink, R. L. C. & Barkema, G. T. Configurational entropy of network-forming materials. *Phys. Rev. Lett.* **89,** 076405 (2002).
2. Mishima, O., Calvert, L. D. & Whalley, E. An apparently first-order transition between two amorphous phases of ice induced by pressure. *Nature* **314,** 76–78 (1985).
3. Meade, C. R., Hemley, J. & Mao, H. K. High-pressure x-ray diffraction of SiO_2 glass. *Phys. Rev. Lett.* **69,** 1387–1390 (1992).
4. McMillan, P. F., Wilson, M., Daisenberger, D. & Machon, D. A density-driven phase transition between semiconducting and metallic polyamorphs of silicon. *Nature Mater.* **4,** 680–684 (2005).
5. Sheng, H. W. *et al.* Polyamorphism in a metallic glass. *Nature Mater.* **6,** 192–197 (2007).
6. Zeng, Q. S. *et al.* Origin of pressure-induced polyamorphism in $Ce_{75}Al_{25}$ metallic glass. *Phys. Rev. Lett.* **104,** 105702 (2010).
7. Ramesh, T. G., Shubha, V. & Ramaseshan, S. Phase transitions in ytterbium under pressure. *J. Phys. F: Metal Phys.* **7,** 981–990 (1977).
8. Zhao, Y. C., Porsch, F. & Holzapfel, W. B. Irregularities of ytterbium under high pressure. *Phys. Rev. B* **49,** 815–817 (1994).

9. Chatterjee, A., Singh, A. K., Jayaraman, A. & Bucher, E. Pressure-induced 4f–5d electron collapse in ytterbium Monotelluride. *Phys. Rev. Lett.* **27,** 1571–1573 (1971).
10. Jayaraman, A., Singh, A. K., Chatterjee, A. & Devi, S. U. Pressure-volume relationship and pressure-induced electronic and structural transformations in Eu and Yb monochalcogenides. *Phys. Rev. B* **9,** 2513–2520 (1974).
11. Zeng, Q. *et al.* Universal fractional noncubic power law for density of metallic glasses. *Phys. Rev. Lett.* **112,** 185502 (2014).
12. Zeng, Q. *et al.* General 2.5 power law of metallic glasses. *Proc. Natl. Acad. Sci.* **113,** 1714–1718 (2016).
13. Chen, D. Z. *et al.* Fractal atomic-level percolation in metallic glasses. *Science* **349,** 1306–1310 (2015).
14. Birch, F., Finite strain isotherm and velocities for single-crystal and polycrystalline NaCl at high pressures and 300 K. *J. Geophys. Res.* **83,** 1257–1268 (1978).
15. Chatterjee, A., Singh, A. K. & Jayaraman, A. Pressure-induced electronic collapse and structural changes in rare-earth monochalcogenides. *Phys. Rev. B* **6,** 2285–2291 (1972).
16. Wendt, H. R. & Abraham, F. F. Empirical criterion for the glass transition region based on Monte Carlo simulations. *Phys. Rev. Lett.* **41,** 1244–1246 (1978).
17. Liu, R. S., Qi, D. W. & Wang, S. Subpeaks of structure factors for rapidly quenched metals. *Phys. Rev. B* **45,** 451–453 (1992).
18. Sheng, H. W., Ma, E., Liu, H. Z. & Wen, J. Pressure tunes atomic packing in metallic glass. *Appl. Phys. Lett.* **88,** 171906 (2006).
19. Lee, G. W. *et al.* Difference in icosahedral short-range order in early and late transition metal liquids. *Phys. Rev. Lett.* **93,** 037802 (2004).
20. Kelton, K. F. *et al.* First x-ray scattering studies on electrostatically levitated metallic liquids: Demonstrated influence of local icosahedral order on the nucleation barrier. *Phys. Rev. Lett.* **90,** 195504 (2003).
21. Syassen, K., Wortmann, G., Feldhaus, J., Frank, K. H. & Kaindl, G. Mean valence of Yb metal in the pressure range 0 to 340 kbar. *Phys. Rev. B* **26,** 4745–4748 (1982).
22. Ziman, J. M. A theory of the electrical properties of liquid metals. I: The monovalent metals. *Philos. Mag.* **6,** 1013–1034 (1961).
23. Hafner, J. Resistivity of liquid, supercooled liquid and amorphous alloys under elevated pressure. *J. Non. Cryst.* Solids **69,** 325–345 (1985).
24. Fritsch, G., Dyckhoff, W., Pollich, W. & Lüscher, E. Dependence on pressure and temperature of the electrical resistivity of the amorphous alloys: Co$_{80}$P$_{20}$ and Pd$_{80}$Si$_{20}$. *J. Phys. F: Met. Phys.* **15,** 1537–1545 (1985).
25. Fritsch, G., Willer, J., Wildermuth, A. & Lüscher, E. Pressure dependence of the electrical resistivity of some metallic glasses. *J. Phys. F: Met. Phys.* **12,** 2965–2974 (1982).
26. Cheung, J. & Ashcroft, N. W. Resistivity of liquid metals under elevated pressure. *Phys. Rev. B* **18,** 559–568 (1978).
27. Hammersley, A. P. FIT2D: a multi-purpose data reduction, analysis and visualization program. *J. Appl. Cryst.* **49,** 646–652 (2016).
28. Chapman, K. W. *et al.* Optimizing high-pressure pair distribution function measurements in diamond anvil cells. *J. Appl. Cryst.* **43,** 297–307 (2010).
29. Qiu, X. J., Thompson, W. & Billinge, S. J. L. PDFgetX2: a GUI-driven program to obtain the pair distribution function from X-ray powder diffraction data. *J. Appl. Cryst.* **37,** 678 (2004).
30. van der Pauw, L. J. A method of measuring specific resistivity and Hall Effect of discs of arbitrary shape. *Philips Res. Rep.* **13,** 1–9 (1958).

Acknowledgements

Author Contributions
H.L., L.L. and R.L. designed all research work; K.C. and P.C. designed PDF work; L.L. and R.L. performed experiments and analyzed data; Q.L. prepared the sample; L.L., Q.L., R.L., H.Z., K.C., P.C., L.W. and H.L. drafted and revised the manuscript.

Additional Information
Competing Interests: The authors declare no competing financial interests.

How to cite this article: Li, L. *et al.* Polyamorphism in Yb-based metallic glass induced by pressure. *Sci. Rep.* **7,** 46762; doi: 10.1038/srep46762 (2017).

Publisher's note: Springer Nature remains neutral with regard to jurisdictional claims in published maps and institutional affiliations.